European Polymer Journal 102 (2018) 151–160

Contents lists available at ScienceDirect

European Polymer Journal

journal homepage: www.elsevier.com/locate/europolj

Synthesis and characterization of a waterborne polyurethane made from castor oil and tartaric acid

M.E. Victoria Hormaiztegui, Mirta I. Aranguren, Verónica L. Mucci*

Instituto de Investigaciones en Ciencia y Tecnología de Materiales (INTEMA), UNMDP, CONICET, Facultad de Ingeniería, Av. Juan B Justo 4302, 7600 Mar del Plata, Argentina

ARTICLE INFO

Keywords:
Bio-based waterborne polyurethane
Castor oil
Tartaric acid

ABSTRACT

Waterborne polyurethanes (WBPUs) based on the reaction of unmodified castor oil (CO) with isophorone diisocyanate (IPDI) were synthesized using dimethylolpropionic acid (DMPA) or tartaric acid (TA) as internal emulsifiers. The effect of the incorporation of TA, a bio-based carboxylic acid, in the synthesis of castor oil-based WBPU was carefully investigated. For comparison, two WBPUs were synthesized using DMPA. The chemical changes that took place during the reaction were followed using FTIR. The raw materials and the final polymeric films were characterized by this technique as well as ^{1}H NMR, XRD, DSC, DMA and TGA. Results indicated that in the case of the sample prepared with TA, the isocyanate reacts with the hydroxyls of the acyl groups of the acid additionally to the alcoholic ones. In all cases, the films prepared by casting were translucent and showed glass transition temperatures above room temperature, although comparatively lower for the WBPU formulated with TA. Differences were also observed in the thermal degradation performance of the films. The observed differences were tracked to those in the molecular structures of the WBPUs.

1. Introduction

Polyurethanes (PU) were first synthesized by Bayer over 75 years ago. Since then and because of the large variety of possible raw materials offering different chemical structures, polyurethanes have been produced with different chemical characteristics, morphologies, and mechanical responses, thus having applicability in many and different industries. PUs can display thermoplastic, elastomeric or thermoset behavior depending on their formulations, in particular the stoichiometry of the isocyanate/OH components, as well as the reaction sequence. Most industrial PUs are synthesized by the polyaddition of polyisocyanates and macropolyols [1,2]. In 2013, the global polymer consumption was 299 million tons, of which 46.3 million tons are due to European consumption and 7.4% of this amount is owed to PU demand [3].

Moreover, the growing consciousness on environmental issues has raised concerns with respect to the use of conventional solvent-borne polyurethanes. These PU formulations are used in industrial applications such as coatings, inks, paints and adhesives, but achieving the final material involves the evaporation of large amounts of volatile organic compounds (VOCs) into the atmosphere, especially during coating application. For this reason, dedicated efforts from both industry and academia have been devoted to reduce the amount of VOCs released into the atmosphere [4–6].

An important progress towards greener PUs was the development of waterborne polyurethanes (WBPU) made by Dieterich et al. [7,8]. WBPUs consist of polyurethane dispersions (PUDs) in which droplets of the polymer (discontinuous phase) are uniformly suspended and stabilized in the liquid medium (continuous phase), which in this case is water [9,10]. It is well known that PUD stability depends strongly on particle size, with average particle size larger than 1000 nm producing sedimentation of the discontinuous phase [11]. On the other hand, Madboury et al. stressed than WBPUs dispersions are stable when the size of PU droplets is between 20 and 200 nm [4].

This kind of aqueous PUDs can be obtained by adding a surfactant to the formulation or by incorporating ionizable chemical groups into the polymer backbone. This last alternative leads to a PU ionomer, in which the ionic groups act as internal emulsifiers. Hence, WBPU dispersions consist of PUs with pendant acid or tertiary nitrogen groups, neutralized to form salts. Depending of the type of ionic groups incorporated to the PU backbone, the PUDs could be of anionic or cationic type [10].

Anionic colloidal PUDs can be synthetized from different raw materials. Generally, these chemical species are a polyol, a diisocyanate, and a dihydroxy acid, such as dimethylolpropionic acid (DMPA), which incorporates a carboxylic functionality in the prepolymer structure.

* Corresponding author.
E-mail address: vmucci@fi.mdp.edu.ar (V.L. Mucci).

https://doi.org/10.1016/j.eurpolymj.2018.03.020
Received 11 October 2017; Received in revised form 9 March 2018; Accepted 12 March 2018
Available online 14 March 2018
0014-3057/ © 2018 Elsevier Ltd. All rights reserved.

Tertiary amine (e.g., triethylamine, TEA) is added to neutralize the carboxylic groups and stabilize the discontinuous phase in water [10]. In this kind of PUDs, ionic centers are placed on the surface of the particle, while the hydrophobic segments, fatty acid from the triacylglyceride, are located in the interior of the particles dispersed in water [12,13].

On the other hand, vegetable oils are one attractive option to replace petroleum based reagents in the synthesis of different polymers. In particular, castor oil (CO) is ideal for the production of PUs [14] because of the presence of hydroxyl groups in its chemical structure that are capable of reacting with isocyanates in the formation of urethane bonds without any previous modification. Like all vegetable oils, CO has the advantages of low toxicity and availability as a renewable resource. These reasons have led to the increasing interest on vegetable oils for the synthesis of bio-polyols that are further used in the synthesis of polymeric materials, such as PUs and WBPUs [15–21].

Frequently, in the synthesis of anionic WBPUs, DMPA is used as the reagent contributing with carboxylic groups. In the present work, a biogenic reagent, tartaric acid (TA), was alternatively used with that aim. TA can be obtained as a by-product from the processing of grapes for wine, and its incorporation in the formulation offers the potential to increase the percentage of bio-based reagents in the synthesized WBPUs [22,23]. For this reason, TA, a cheap, natural and easily accessible reagent [24], has been utilized in the preparation of tartrate derivatives, which were then used to formulate PUs [24–27]. The use of this bio-based acid in the synthesis of WBPUs has been considered by some authors, such as Gündüz and Gafarogullari [12]. They prepared WBPUs using a triol, toluene diisocyanate (TDI), TEA and ethylene diamine, and compared the use of TA and DMPA as carboxylic acids [12]. However, in that case, they used a synthetic triol, while in the present work, TA was used to develop a vegetable oil-based WBPU, thus achieving a relatively high content of bio-based reagents. Additionally, the influence of DMPA content in a series of castor oil based WBPUs was investigated. Thus, WBPUs based on DMPA and CO with two different ratios of CO/DMPA were prepared. IPDI was the diisocyanate used for providing transparent films for use as coatings and TEA was used as aiding agent in the dispersion of the PUs containing carboxylic acids.

2. Experimental part

2.1. Raw materials

Isophoronediisocyanate (IPDI, 98% purity, f = 2), triethylamine (TEA, 99% purity), dibutyltindilaurate (DBTDL, 95% purity), dimethylolpropionic acid (DMPA, 98% purity, f = 2), dimethylformamide (DMF) and acetone were all purchased from Sigma-Aldrich Corp. and used without purification. L-(+)-Tartaric acid (TA, 98% purity, f = 2) was purchased from BioPack S.R.L. The two carboxylic acids were dried under vacuum before use.

Castor oil (CO, supplied by Parafarm®, OH number = 177.21 mg of KOH/g, Iodine value = 82.36 g I_2/100 g according to Wijs method [28], f = 2.9), which was used as the reagent contributing with OH groups, was dried under vacuum before use.

The chemical structures of the main reagents are shown in Fig. 1.

2.2. Synthesis of WBPU

CO (14 g) and DMPA (OH equivalent molar ratio of CO to DMPA = 1.0) were mixed in a 250 ml glass five necked flask equipped with a condenser, a mechanical stirrer and a nitrogen inlet to ensure a flow of this gas that helped to reduce the formation of urea bonds with atmospheric humidity. DMPA was previously dissolved in dimethylformamide (DMF) with the aim of facilitating dispersion in the oil (30% wt./vol.). IDPI (NCO/OH ratio = 1.4) and DBTDL (1 wt% with respect to the total reaction mass) were added and the reaction proceeded for 5 h at 78 °C [4]. During this reaction step, the viscosity increased, but it was maintained at the desired level by the addition of acetone (20 ml of acetone were initially added and then the volume of the reacting mixture was kept constant by replacing the evaporated solvent). After the polymerization step was completed, the temperature was reduced to 60 °C and TEA was added (equimolar ratio with DMPA) Vigorous stirring (800 rpm) was used in order to disperse the product in distilled water and finally, rotary vacuum evaporation at 30 °C was used to remove any remaining solvent. The waterborne polyurethane was coded WBPU-DMPA 1 eq.

Other PU samples were prepared using an OH equivalent molar ratio of CO to DMPA = 0.8, maintaining the NCO/OH ratio = 1.4, to compare the effect of the acid-diol concentration on the properties of the WBPU obtained. This polyurethane was named WBPU-DMPA-0.8 eq.

However, the most interesting change of the formulation was the replacement of the carboxylic acid, DMPA by TA. The synthesis was carried out in two steps to control the fast reaction of TA with the isocyanate: CO and IPDI were added into the reactor in the first step at 78 °C for 2 h 30 min under N_2 atmosphere. TA dissolved in DMF (30% wt./vol.) was added and the reaction continued for 2 h. For this particular sample, an equivalent ratio of NCO/OH = 1.6 was used for the preparation of non-brittle, self-standing films. As it will be further discussed, the TA can react with the IPDI with a functionality greater than the nominal f = 2, thus supporting the use of a higher (nominal) isocyanate ratio. Then, the temperature was set at 60 °C and TEA was added while continuing the stirring (equimolar ratio of −COOH with TEA). 100 ml of distilled water were added under vigorous stirring in order to disperse the PU that was coded WBPU-TA 0.8 eq [12].

In all cases the final aqueous dispersions of the WBPU prepared were concentrated to solid content of 27–32 wt%.

Table 1 summarizes the reaction conditions for the synthesis of the polyurethanes.

The films of WBPUs were prepared by casting of the dispersions in glass Petri dishes coated with non-stick adhesive paper and further evaporation of the water solvent at 30 °C overnight in a convection oven.

2.3. Characterization

2.3.1. FTIR analysis

ATR-FTIR spectroscopic analysis was performed using a Bruker IFS 25 spectrometer at ambient temperature. An ATR sampling accessory with a ZnSe crystal was used to characterize the WBPUs films. Additionally, transmission FTIR spectra were obtained from uncompletely reacted samples collected during the synthesis of the WBPU-TA. All spectra were the average of 64 scans obtained at a resolution of 4 cm^{-1} within the range of 400–4000 cm^{-1}. To study the NH and the C=O stretching regions in all samples, deconvolution of the absorption peaks and curve-fitting of those regions were performed using OriginPro 8.5 software. The deconvolution was performed assuming Gaussian peaks [29].

2.3.2. Nuclear Magnetic Resonance Spectroscopy (^{1}H NMR)

The ^{1}H NMR spectra of the WBPU films were recorded in a Spectrometer Bruker Avance II 500 (500 MHz). The samples were dissolved in dimethyl sulfoxide for 2 h within an ultrasonic bath at 40 °C. The spectra were acquired in the range of −2 to 10 ppm.

2.3.3. Dynamic light scattering (DLS)

The average particle size and particle size distribution of the WBPU dispersions were measured by dynamic light scattering using a Malvern Zetasisernano S-90 with a laser beam of 632 nm (Malvern Instruments Co. Ltd., Worcestershire, United Kingdom) at 25 °C. The samples were diluted in deionized water before the measurement (2.5 %wt/vol).

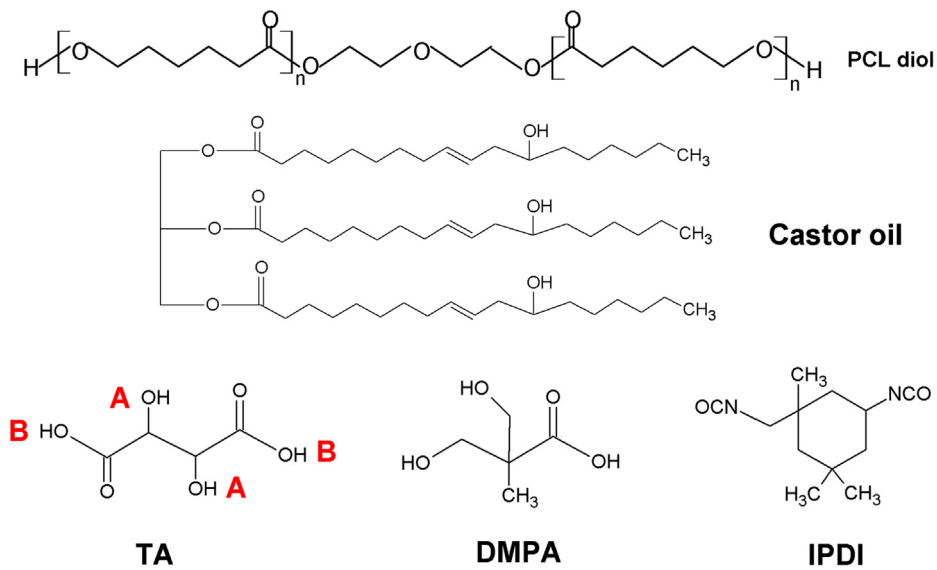

Fig. 1. Chemical structures of the main reagents.

Table 1
Reaction conditions of WBPUs.

Sample	Time and steps	Equivalent ratios		
			NCO/OH	Acid/TEA
WBPU-DMPA 1 eq	5 h 1 step	CO/DMPA = 1.0	1.4	1.0
WBPU-DMPA 0.8 eq	5 h 1 step	CO/DMPA = 0.8	1.4	1.0
WBPU-TA 0.8 eq	2.5 h and 2 h 2 steps	CO/TA = 0.8	1.6	1.0

2.3.4. X-ray diffraction (XRD)

X PANalytical X'Pert PRO X-ray diffractometer (Cu Kα radiation with wavelength: 1.54187 Å) was used to obtain the X-ray diffraction spectra. The measurements covered a range of diffraction angles from 5° to 60° and were performed at a scanning speed of 0.016° s^{-1}.

2.3.5. Differential scanning calorimetry (DSC)

A differential scanning calorimetry (DSC) Pyris 1 Perkin Elmer equipment, provided with an electric intracooler as refrigerator unit was used to obtain the thermograms of the WBPUs. The samples were scanned from −70 °C to 200 °C at 10 °C/min under N_2 or air atmosphere.

2.3.6. Thermal gravimetric analysis (TGA)

Thermogravimetric curves were obtained with a TGA-50 Shimadzu. The essays were run from room temperature to 700 °C at 10 °C/min under N_2 atmosphere.

2.3.7. Dynamic mechanical analysis (DMA)

An Anton PaarPhysica MCR 301 Rheometer was used to measure the viscoelastic properties of the samples. The samples were characterized using dynamic torsion of solid rectangular bars in the temperature range from -80 to 140 °C, at a scanning rate of 5 °C/min and in the range of linear viscoelastic behavior of the samples (constant strain of 0.05%, frequency of 1 Hz).

3. Results and discussion

3.1. Structures of the WBPUs: FTIR and ^{1}H NMR analysis

Infrared spectroscopy was used to evaluate the success of the synthesis of the WBPUs through the assignment of the functional groups present in the PU films and comparison with those present in the starting reagents.

Fig. 2 shows the spectra of the CO and the WBPU films obtained from this vegetable oil. The intensity of the peak at 3408 cm^{-1} corresponds to the main band of the OH groups of CO. This band is absent in the WBPUs spectra, while a more intense and narrow band appears around 3300 cm^{-1} corresponding to the stretching vibration −N−H of the urethane bonds.

The absorption corresponding to the insaturations in the oil can be seen in the spectra of CO in Fig. 2 at 3009 cm^{-1}. The iodine value of CO (82.36 g I_2/100 g oil, as reported in the Experimental section) corresponds to three C=C bonds in the CO molecular structure, in good agreement with the bibliography [30,31].

Strong new bands appear, such as the amide-II band at 1540 cm^{-1} (contribution of −NH in-plane bending and C−N stretching) [32,33], the carboxyl stretching vibration in the amide-I region at 1630–1730 cm^{-1}, the region at 1210–1240 cm^{-1} from the stretching vibration of the C=O group of urea combined with the −N−H group,

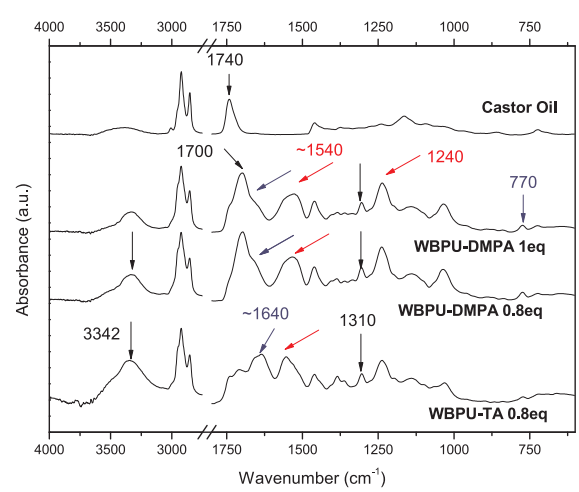

Fig. 2. FTIR spectra of CO and CO-derived WBPUs films.

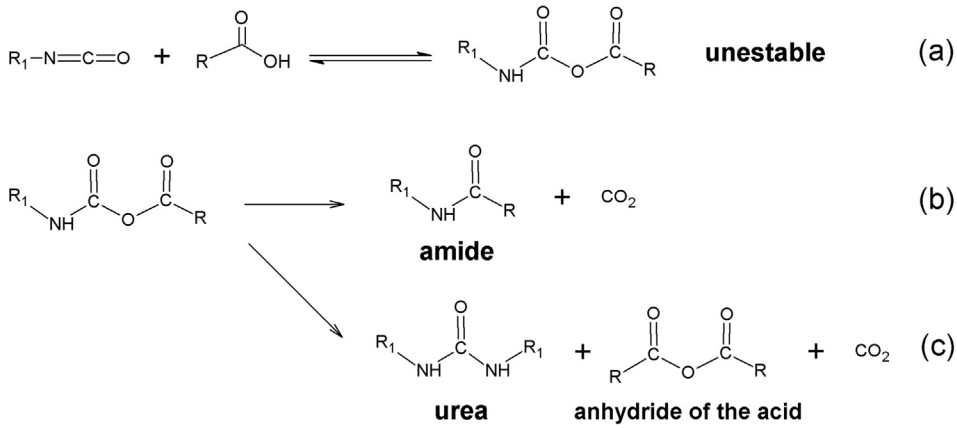

Fig. 3. Isocyanate-carboxylic acid reaction.

and the band at 773 cm^{-1} due to the carboxylic ion (−COO^-) [33–36]. The absorption at 1730–1745 cm^{-1} corresponds to the absorption of carboxyl groups of the ester groups in the CO and is partially overlapped with the absorption of the carbonyl of urethane.

On the other hand, the WBPU-TA spectrum shows a more intense peak from the NH stretching vibration at 3342 cm^{-1} and a new strong absorption band at 1640 cm^{-1}. These differences suggest that the OH belonging to the acid group in the tartaric acid molecule can also react with the isocyanate groups to form amide groups, as it will be further discussed, Fig. 3 [37].

Blagbrough et al. studied the condensation reaction between isocyanates and carboxylic acids. These authors found that aliphatic isocyanates react easily with carboxylic acids producing an intermediate, mixed carboxy-carboxylic anhydride, which is not stable under the reaction conditions (Fig. 3a) [38]. Additionally, Sorenson in 1959, found that the decomposition of the intermediate can follow two paths and both involve the production of CO_2. In the first one, the sub-product is an amide (Fig. 3b), while the second path produces an urea and an anhydride (Fig. 3c) [39]. From our results, it is clear that the reaction between IPDI and TA carboxylic acid is produced by the mechanism (b) since the band corresponding to the asymmetric stretching of the C=O group of the anhydride (between 1800 and 1840 cm^{-1}) [40] is not observed and this is explained by steric impediments. On the other hand, according to reports in the bibliography, in the solid phase, secondary amides absorb strongly at 1680–1630 cm^{-1} due to the stretching vibration C=O, as it is observed in the reacted films [40].

In case of synthesis with DMPA, the probability of reaction of the IPDI with the carboxylic acid of DMPA compared to that of reaction with the hydroxyl groups of the molecule is 1–2, whereas in the TA that ratio is 1–1, because of this, the probability that the reaction occurs between IPDI and COOH is higher in the WBPU-TA. In addition, the carboxylic group of DMPA is sterically more hindered than those of TA, which is another reason for a larger probability of this reaction in WBPU-TA than in WBPU-DMPA [12].

In order to monitor the progress of the reaction over time, samples were taken during the synthesis and analyzed by FTIR.

Fig. 4 shows the spectra of the samples collected at different reaction times and the final film of WBPU-TA, in the area of the characteristic vibration of the isocyanate group (−NCO): 2250 cm^{-1}. It can be seen that the band decreases with time as a consequence of the reaction. In the first part of the reaction, a moderate decrease in the peak is observed, attributed to the fact that the source of OH in the reaction medium is castor oil, whose secondary hydroxyls have low reactivity. At 2 h 30 min of reaction the TA is added, and from that moment the IPDI can react with both alcohol functional groups: the hydroxyl groups of CO and/or TA, and with the hydroxyl groups of the carboxylic acid functional groups of TA (Fig. 3) [39,40]. This last reaction takes place quickly, which is evident in the spectrum taken at 2 h 45 m (pink curve,

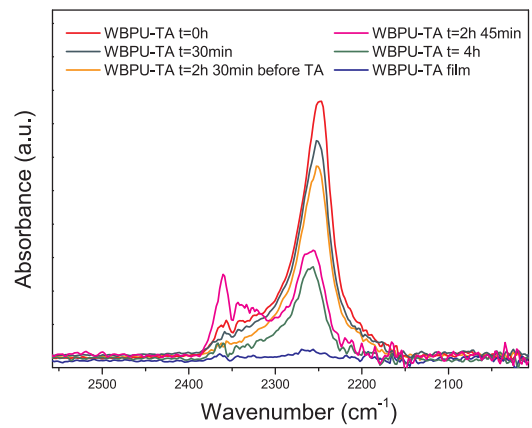

Fig. 4. FTIR spectra of samples taken during the synthesis of WBPU-TA in the area of the characteristic vibration of the isocyanate group −NCO.

Fig. 4), where it can be observed that an important consumption of IPDI has occurred in a short period of time. The hypothesis that the IPDI reacts with the OH of the acid group in addition to the OH group of alcohol is confirmed by the presence of the peak that appears at 2360 cm^{-1}, assigned to CO_2, which is one of the products that is generated in the proposed reaction, as illustrated in Fig. 3b. After 4 h of reaction, the IR absorption of CO_2 is again negligible, which indicates that the reaction of the IPDI with the OH of the acid has been completed. The remaining isocyanate is the excess, which finally reacts to give ureas when water is added to obtain the dispersion; so the peak is not present in the film's spectrum.

On the other hand, Fig. 5 shows the progress of the reaction before adding the TA and the film spectrum for the region between 3750 and 3500 cm^{-1} (Fig. 5a) and for the acyl group region (Fig. 5b), which are the regions where major changes occur during the reaction.

In the spectra of Fig. 5a, the appearance of the band at 3375 cm^{-1} can be observed when comparing the spectrum obtained at the beginning of the reaction (t = 0) and the one measured just before adding the TA (t = 2 h 30 min). This band is attributed to the stretching −N−H of the urethane formed due to the reaction between CO and IPDI, the only reagents present in the medium before the addition of TA. In the final film, the peak is slightly shifted towards lower wavenumbers, due to the contribution of the −N−H groups of the amides formed and the hydrogen bonds that are generated.

Finally, in Fig. 5b, the changes in the C=O region are shown. At time zero, the band observed at 1742 cm^{-1} corresponds to the ester group of CO. As the reaction progresses, a more intense band appears at 1711 cm^{-1} corresponding to the acyl of the urethane group formed. In the spectrum of the film, the band of 1630 cm^{-1} associated with the

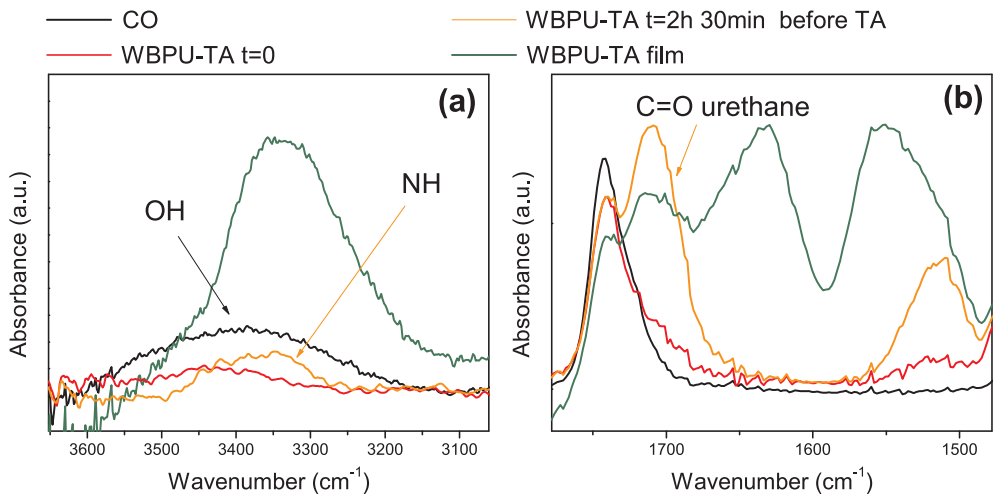

Fig. 5. FTIR spectra of samples of WBPU-TA during the reaction, before adding the TA for the region between 3750 and 3500 cm^{-1} (a) and for the acyl group region (b).

amides can also be seen, which, as previously analyzed, is a product of the reaction between the TA and the IPDI.

Because TA is added as a solution in dimethylformamide (DMF), it is not possible to analyze the regions where the solvent has very strong absorption bands. In particular, DMF shows a very intense band in the region of C=O absorption. Fig. S1 of supporting information shows the FTIR spectra of DMF, of the mixture at an advanced time of reaction and of the final film. The comparison of the spectra is useful to confirm the complete evaporation of the DMF during the processing that ends with the casting of the film and to understand the impossibility of analyzing the progress of the polymerization using the FTIR region 1400–1800 cm^{-1} when the DMF is still present in the reaction mixture.

Fig. 6 shows the structure representative for the reaction between CO and IPDI were ***R*** could be another molecule of CO or the acid, DMPA or TA. In the case of TA two possible reactions can take place, according to the discussion above.

The analysis of the FTIR spectra between 3000 and 3800 cm^{-1} and 1600 and 1800 cm^{-1} were performed by deconvolution of the absorption bands in those regions. The deconvolution curves are shown as supplementary information (see SI, Fig. S2) and Table 2 summarizes the results in terms of percentage of area (relative values) and peak assignments. The peak position used as internal reference to normalize the FTIR spectra was at 1744 cm^{-1} [20,32,33,41–46].

The percentage of -N-H involved in H-bonds is higher in WBPU-TA than in the other two WBPUs probably because that PU has a higher NCO/OH ratio, leading to a higher concentration of urethane and amide groups formed by the reaction of TA with IPDI.

The percentage area corresponding to the esters groups of the CO in WBPU-DMPA's (see SI, Fig. S2) corresponds to 4% of the total C=O area while for the WBPU-TA this area increases to 6%, which coincides with the relative reduction of the contribution of the urethane peak (1703 cm^{-1}), and appearance of the band in 1626 cm^{-1} corresponding to the amide formation.

In Table 2, the area corresponding to the ester groups was eliminated and the contribution of the areas of the rest of the peaks of the region (which corresponds to groups formed by reaction) were normalized to 100. The values reported are to be considered estimations of the relative contributions of the particular bands of the region, facilitating the comparison between the different WBPUs synthesized.

In the polyurethanes obtained from DMPA no changes were observed in the contributions of the areas centered at 1703 cm^{-1} and 1652 cm^{-1}, corresponding to urethane and ureas groups, respectively.

From the comparison of the results obtained for WBPU-DMPA 0.8 eq and WBPU-TA 0.8 eq, it is seen that there is a decrease in the contribution to acyl groups of urethane, at the same time that the absorption of amide groups appears in the spectrum of the last one. Additionally, since the WBPU-TA 0.8 eq is formulated with a higher NCO/OH ratio, an increase in the band 1652 cm^{-1} is also observed (from ureas formed with the excess of NCO during the dispersion of the polymer in water). However, it is important to notice that although the nominal NCO/OH ratio is higher in this case, the additional reaction of the isocyanate with the OH of the acid group results in a lower than

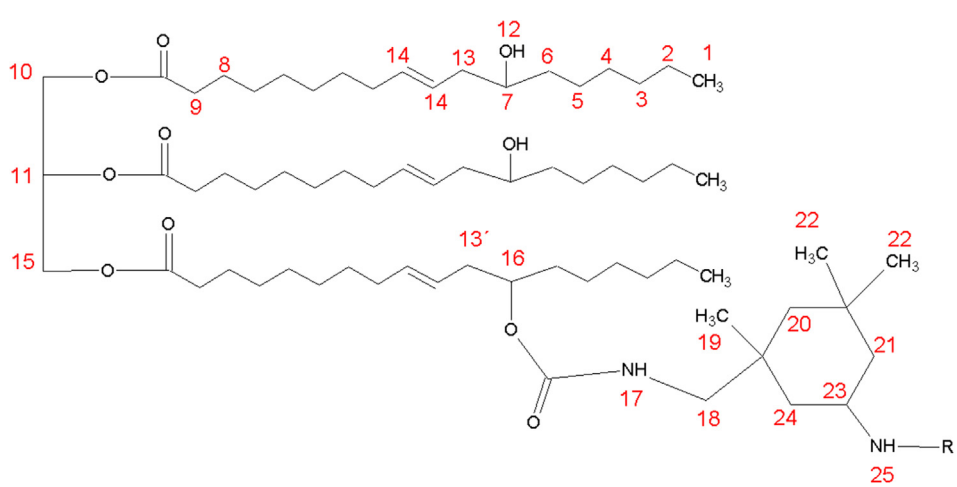

Fig. 6. Example of possible chemical structures obtained in the synthesis of the WBPUs.

Table 2
Results from the deconvolution of the FTIR absorption bands of the WBPUs films.

Sample	−N−H region		C=O region		
	H-bonded 3335–3340 cm^{-1} % of area	Free 3533–3537 cm^{-1} % of area	Peak position (cm^{-1}) 1703 % of area	1652 % of area	1626 % of area
WBPU-DMPA 1 eq	85.4	14.6	85.1	14.9	–
WBPU-DMPA 0.8 eq	82.3	17.7	85.7	14.3	–
WBPU-TA 0.8 eq	89.6	10.4	55.9	21.5	22.5

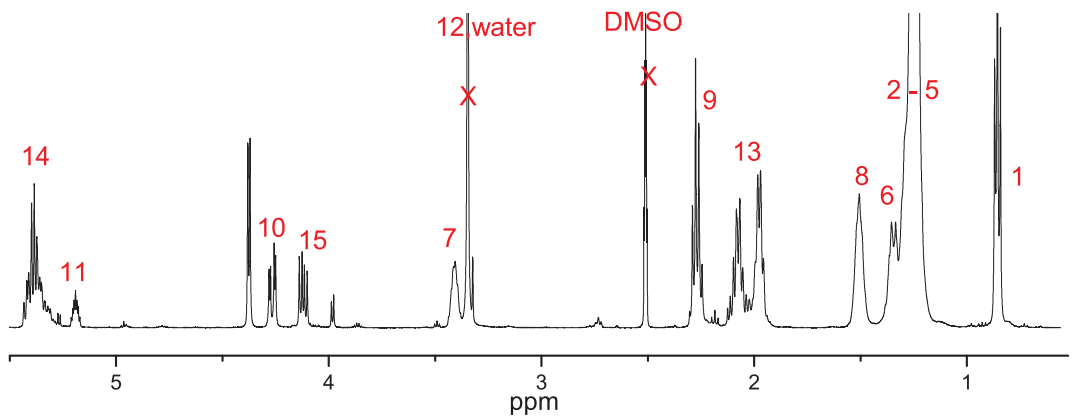

Fig. 7. ^{1}H NMR of the castor oil.

nominal excess of isocyanate.

Fig. 7 shows the ^{1}H NMR of the CO, numbers in red correspond to the schematic structure of the unreacted vegetable oil (partially shown in Fig. 6).

In Table 3 the peaks assignment is summarized [20,46–50]. The peak area assigned to the protons of terminal methyl groups was taken as the basis for the calculation.

The results show that the fatty acid composition is very high in ricinoleic acid, as can be deduced from the relative concentration of protons coded 7 and 14 in the Table 3 (the H attached to the carbon atom linked to the hydroxyl group and the protons involved in the unsaturation). The results are in agreement with the measured OH value and the iodine value already reported in this work. The peak at 3.4 ppm was not assigned and may be related to some unaccounted impurity present in the sample.

The ^{1}H NMR spectra of the rest of the raw materials, as well as those of the salts prepared from the acid molecules (TA and DMPA) and TEA were also recorded and are presented as supplementary material (see SI, Figs. S3–S7).

The ^{1}H NMR spectra of the WBPU films are much less cleaner than those of the original monomers (Fig. 8). However, some peaks can be used to confirm the presence of the different components in the final polyurethane structure.

The analysis of the WBPU-DMPA samples shows that the region of 0 to 1.5 ppm is very crowded with the signals from protons of CH_2 and CH_3 from CO, DMPA, and IPDI. However, the peak due to CH_3 in CO still appears at 0.88 ppm and the one corresponding to the CH_2 still appears at 1.25 ppm, although superposed to other signals (notice the double peak at 1.25 and multiple peaks at ~1 ppm).

The singlet of the protons coded as 18 in the IPDI segment of the molecular structure can be seen in the spectra of the polymers, but shifted towards lower ppm because of the neighboring NH of the urethane groups (Fig. 6). It is also interesting that two different singlets appears (2.75 and 2.9 ppm instead of the singlet at 3.4 ppm that corresponds to the protons coded as 18 of the IPDI) suggesting different surroundings, probably due to reaction with CO or with DMPA.

Comparing the two formulations of WBPU-DMPA, the one coded as 0.8 eq contains comparatively more DMPA and more IPDI (taking the CO as the basis for the comparison). Correspondingly, in the spectrum of this sample, the peaks of IPDI appear larger and there are also some

Table 3
Peaks assignment of ^{1}H NMR of the castor oil.

	Assignment	ppm	multiplicity	H theoretical	H experimental
1	methyl protons at the end of the fatty acid chains	0.86	Triplet	9	9
2–5	$-CH_2-$ separated by at least one carbon from the unsaturation, or the carbon with the hydroxyl group or the ester group	1.26	Multiplet	48	49.48
6	between the carbon with the hydroxyl group and the free end of the fatty acid chain	1.35	Quadruplet	6	5.53
7	−CH− attached to the C with the −OH group	3.41	Multiplet	3	3
8	$-CH_2-$ separated by one carbon from the ester group	1.51	Multiplet	6	6.11
9	$-CH_2-$ neighbor to the ester groups	2.27	Triplet	6	6.18
10 and 15	$-CH_2-$ of the glycerol part of the castor oil	4.11 and 4.27	Doublet	4	3.33
11	−CH− of the glycerol part of the castor oil	5.19	Multiplet	1	1.41
13	$-CH_2-$ close to the carbon-carbon unsaturation	1.97–2.18	Multiplet	12	11.48
14	vinyl groups	5.25–5.43	Quintuplet	6	5.65
TOTAL				**101**	**101.17**

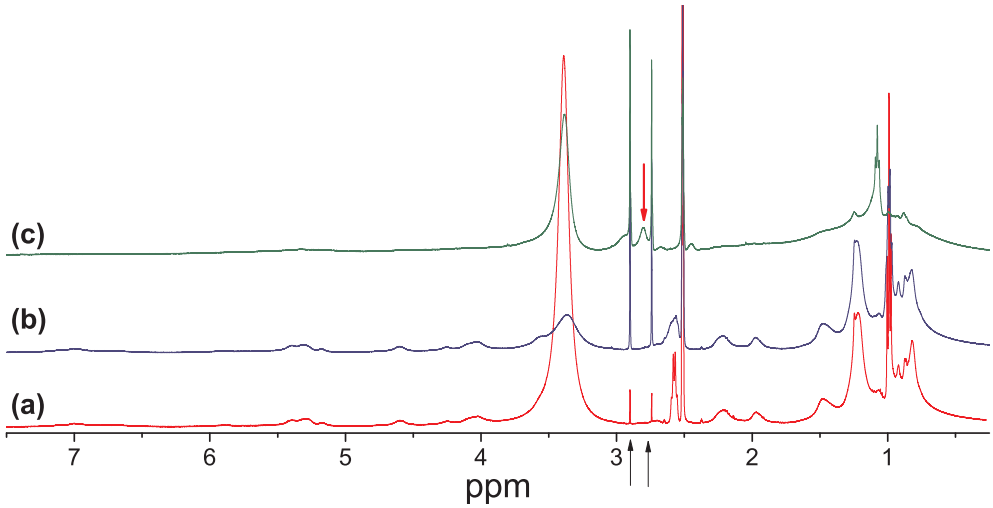

Fig. 8. ^{1}H NMR of the WBPU films (a) WBPU-DMPA 1 eq, (b) WBPU-DMPA 0.8 eq and (c) WBPU-TA 0.8 eq.

differences in the relative height of the signals in the CH_2 and CH_3 region.

Finally, the TEA added to stabilize the suspension also presents peaks at 1.25 and 3.2 ppm (the spectra of the salts formed between the carboxylic acid and TEA are included in the supplementary material S7).

Regarding the spectra of the WBPU-TA, as in the case of the DMPA samples, two singlets at 2.75 and 2.9 ppm appear that correspond to the reacted IPDI. However, in this case, the spectrum shows very broad peaks that difficult further assignments. Nevertheless, the peak centered in 2.80 ppm (pointed with a red arrow) corresponds to the OH group of TA indicated with the letter **A** in Fig. 1.

3.2. Characterization of the WBPUs dispersions

As previously mentioned, particle size between 20 and 200 nm and pH values > 7 have been reported to lead to a stable dispersion of commercial and laboratory formulations of anionic WBPUs [4,51–57].

In Table 4 particle size and pH values of the synthetized WBPUs are summarized. Dispersions with particle size below 40 nm were obtained. This was achieved by adjusting the stirring parameters in the reactor such as stirrer height, size of the blades, speed, amount of added water and rate of its addition. The pH values of the final WBPU dispersions were in the range of 8–9. At this pH range, the dispersions are stable due to the presence of $-COO^-$ groups in the hydrophilic moieties of the carboxylic acid (DMPA or TA). Also, because of the presence of these groups, the micelles become negatively charged and repel each other, contributing to obtain a uniformly dispersed PU [56]. Hence, the synthesized WBPUs comply with both premises (pH values and particle size), resulting in the dispersions being stable. Experimentally, there was no evidence of precipitate even after 12 months.

3.3. Characterization of the WBPUs films

Fig. 9 exhibits the X-ray diffractograms in the range of 2θ = 5–40° for all the castor oil based WBPUs synthesized. XRD patterns of the polyurethanes display only a broad peak centered at 2θ ~ 18° for all samples [9,20,38,58]. In other words, these WBPUs do not present an organized crystalline phase, in agreement with the visual observation of transparency for the three samples, characteristic of amorphous materials.

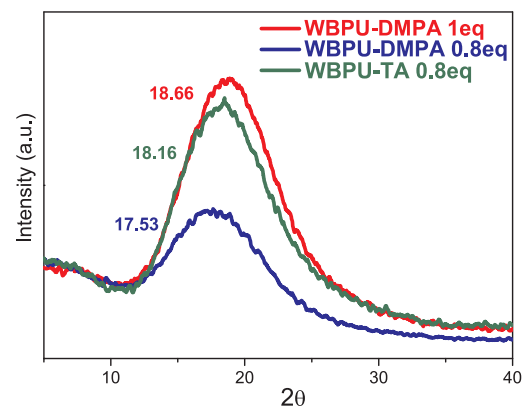

Fig. 9. XRD patterns of WBPUs samples.

Table 5 shows DSC results for all the WBPU synthesized, where it can be seen that no melting event appears in the DSC traces of any of the PU, in agreement with published results [20,59–61], and with the above XRD results. On the other hand, all PU showed a T_g above room temperature, thus, resulting in materials with low flexibility. Values of Tg higher than room temperature are characteristic of crosslinked polyurethanes (as for example in the case of PU rigid foams, and in particular they have been reported in the case of several derived biopolyurethanes) [61–65]. This feature is the result of the functionality of the biopolyol (f > 2) and its relatively low molecular weight. Additionally, and comparatively, the sample WBPU-DMPA 0.8 eq contains a lower concentration of CO than WBPU-DMPA 1 eq in its structure. In the latter, there is a higher concentration of the trifunctional oil molecule (which would lead to a higher crosslinking density), but this also means a higher concentration of pendant chains in the molecular

Table 4
Properties of WBPUs dispersions.

Sample	Mean particle size (nm)	pH
WBPU-DMPA 1 eq	26.2 ± 0.9	8.92
WBPU-DMPA 0.8 eq	27.7 ± 0.5	8.49
WBPU-TA 0.8 eq	39.4 ± 4.6	8.06

Table 5
Properties of WBPUs films.

Sample	T_g (DSC, °C) Mid-point	T_g (DMA,°C) tan δ
WBPU-DMPA 1 eq	53	40
WBPU-DMPA 0.8 eq	55	42
WBPU-TA 0.8 eq	48	37

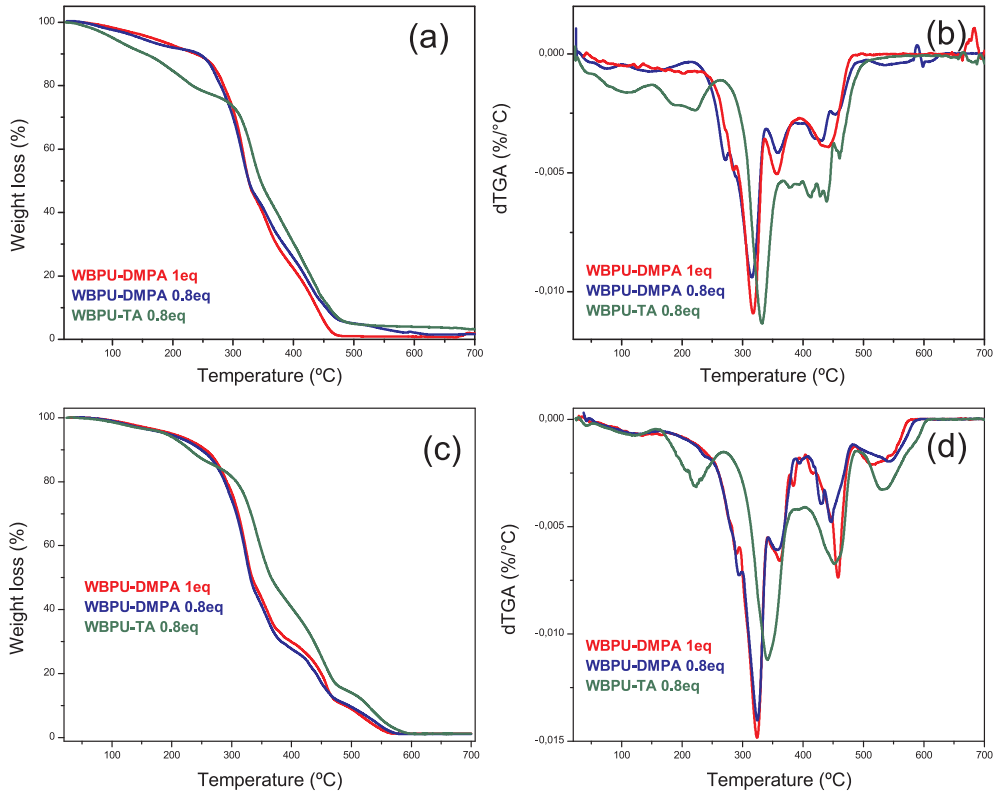

Fig. 10. (a) TG curves and (b) dTGA curves of the samples under N_2 atmosphere, (c) TG curves and (d) dTGA curves of the samples in air atmosphere.

structure and these act as internal plasticizers. This effect was dominant and the Tg of WBPU-DMPA 1 eq resulted slightly lower than that of WBPU-DMPA 0.8 eq (DSC and DMA results).

The T_g values obtained from the peak of tan δ (DMA results, see SI Fig. S8) are reported in Table 5 and show the same trend observed from the DSC values, although the absolute values differ, as it is usually observed [66]. In this particular case, lower values of Tg were measured from DMA because of the lower heating speed used in the test.

TGA and dTG curves for the WBPUs synthesized are shown in Fig. 10, and degradation temperatures at which the weight sample loss equals 5, 50 and 90% of the initial one (T_5, T_{50} and T_{90}) are reported in Table 6.

The studied CO-based WBPUs thermally degrade in three main steps. The first step involves around 20–30% of weight loss, and the last two steps the remaining 80–70%.

The main degradation of all the samples (N_2 atmosphere) occurs in the region 250–350 °C. However, WBPU-TA has lower thermal stability than the other two samples and degradation begins at lower temperature [12]. A comparison of the thermal decomposition of the salts formed from DMPA and from TA with TEA (not included) showed that the decomposition takes place in the low range of temperatures observed and that the degradation of the TA-TEA salt begins about 80 °C below that of DMPA-TEA. Thus, it is proposed that the initial difference observed in the thermal degradation of the WBPUs is due to the elimination of the amines forming salts that stabilized the PUs. As mentioned above, the main degradation peak at about 300 °C is due to the decomposition of the urethane bonds [56,62,63], closely followed by further degradation of the biopolyol [62,64]. Finally, above 400 °C the degradation of the previously formed fragments takes place [56,62,64]. The final char is negligible for all the materials [67–69].

In the Fig. 10c and d, the results of the thermal degradation in air atmosphere are also included. The explanation is similar to that given above for the degradation in N_2 atmosphere, except that higher thermal stability is displayed in air. This is the result of the polymerization of the remaining double bonds of the castor oil due to the action of the oxygen in the air. The oxypolymerization of unsaturated vegetable oils is well known and it has been analyzed before in the literature [70,71]. Because of the action of the oxygen, there is no remaining char.

Table 6
Degradation temperatures of the different PUs in N_2 atmosphere.

Sample	Temperature (°C) for weight loss of 5%, 50% and 90%			T_{dmax} (°C)
	T_5	T_{50}	T_{90}	
WBPU-DMPA 1 eq	166.9	325.7	338.7	318.2
WBPU-DMPA 0.8 eq	146.5	325.7	353.8	315.6
WBPU-TA 0.8 eq	100.8	345.6	459.5	332.5

4. Conclusions

WBPU could be synthesized with a relatively high carbon content coming from the biomass, by replacing the dimethylolpropionic acid, most commonly used for the synthesis of this type of matrices, with tartaric acid, derived from the wine-grape process.

The analysis of the experimental results indicates that TA reacts with the isocyanate through the hydroxyl groups corresponding to the alcoholic and acid groups. The films obtained from this acid are transparent and their Tg value is above room temperature as it is also the case of the DMPA derived WBPUs. However, the Tg is about 10 °C lower in the case of the TA formulated WBPUs, which may be an advantage for obtaining more flexible materials. This will be part of the ongoing study on the physical properties of the materials as films and coatings.

Finally, although the thermal degradation of the TA-derived film begins at lower temperature, it is more thermally stable in the high temperature range.

Overall, the possibility of replacing DMPA with a bio-based di-

dhydroxyl carboxylic acid in the formulation of a WBPU, allows synthesizing a prepolymer with different chemical structure. The new synthesis leads to stable dispersions and films with glass transition temperature slightly above room temperature, and with higher carbon content derived from biomass (38 wt% and 43 wt% in DMPA- and TA-based formulations, respectively).

Acknowledgements

The researchers thank CONICET (PIP 0866), ANPCyT (PICT140732) and UNMdP (15/G430-ING436/15) for their financial support. M.E.V. Hormaiztegui thanks CONICET for a fellowship grant.

Appendix A. Supplementary material

Supplementary data associated with this article can be found, in the online version, at https://doi.org/10.1016/j.eurpolymj.2018.03.020.

References

[1] H.W. Engels, H.G. Pirkl, R. Albers, R.W. Albach, J. Krause, A. Hoffmann, H. Casselmann, J. Dormish, Polyurethanes: versatile materials and sustainable problem solvers for today's challenges, Angew. Chemie Int. Ed. 52 (36) (2013) 9422–9441.
[2] G. Avar, U. Meier-Westhues, H. Casselmann, D. Achten, Polyurethanes vol. 10, (2012).
[3] PlasticsEurope, Plastics – The Facts 2014/2015: An Analysis of European Plastics Production, Demand and Waste Data, PlasticsEurope, 2015, pp. 1–34.
[4] S.A. Madbouly, Y. Xia, M.R. Kessler, Rheological behavior of environmentally friendly castor oil-based waterborne polyurethane dispersions, Macromolecules 46 (11) (2013) 4606–4616.
[5] S. Gogoi, N. Karak, Biobased biodegradable waterborne hyperbranched polyurethane as an ecofriendly sustainable material, ACS Sustain. Chem. Eng. 2 (12) (2014) 2730–2738.
[6] K.L. Noble, Waterborne polyurethanes, Prog. Org. Coat. 32 (1997) 131–136.
[7] D. Dieterich, W. Keberle, H. Witt, Polyurethane ionomers, a new class of block polymers, Angew. Chemie Int. Ed. Engl. 9 (1) (1970) 40–50.
[8] D. Dieterich, Aqueous emulsions, dispersions and solutions of polyurethanes; synthesis and properties, Prog. Org. Coat. 9 (3) (1981) 281–340.
[9] S.A. Madbouly, J.U. Otaigbe, Recent advances in synthesis, characterization and rheological properties of polyurethanes and POSS/polyurethane nanocomposites dispersions and films, Prog. Polym. Sci. 34 (12) (2009) 1283–1332.
[10] D.K. Chattopadhyay, K.V.S.N. Raju, Structural engineering of polyurethane coatings for high performance applications, Prog. Polym. Sci. 32 (3) (2007) 352–418.
[11] M.V. Ebrahimi, M. Barikani, S. Mohammad, S. Mohaghegh, Polyurethane dispersions: influence of polyol, Iran. Polym. J. 15 (4) (2006) 323–330.
[12] G. Gündüz, M. Gafarogullari, Highly branched and tartaric acid-based water-borne resins, J. Appl. Polym. Sci. 80 (4) (2001) 604–612.
[13] K. Mequanint, R. Sanderson, Hydrolytic stability of nano-particle polyurethane dispersions: Implications to their long-term use, Eur. Polym. J. 42 (5) (2006) 1145–1153.
[14] C. Zhang, T.F. Garrison, S.A. Madbouly, M.R. Kessler, Recent Advances in Vegetable Oil-Based Polymers and Their Composites, Elsevier B.V., 2017.
[15] A. Noreen, K.M. Zia, M. Zuber, S. Tabasum, A.F. Zahoor, Bio-based polyurethane: an efficient and environment friendly coating systems: a review, Prog. Org. Coat. 91 (2016) 25–32.
[16] X. Kong, L. Zhao, J.M. Curtis, Polyurethane nanocomposites incorporating biobased polyols and reinforced with a low fraction of cellulose nanocrystals, Carbohydr. Polym. (2016).
[17] S. Saalah, L.C. Abdullah, M.M. Aung, M.Z. Salleh, D.R. Awang Biak, M. Basri, E.R. Jusoh, Waterborne polyurethane dispersions synthesized from jatropha oil, Ind. Crops Prod. 64 (2015) 194–200.
[18] H.K. Shendi, I. Omrani, A. Ahmadi, A. Farhadian, N. babnejad, and M. R. Nabid, Synthesis and characterization of a novel internal emulsifier derived from sunflower oil for the preparation of waterborne polyurethane and their application in coatings, Prog. Org. Coat. 105 (2017) 303.
[19] P.N. Moghadam, M. Yarmohamadi, R. Hasanzadeh, S. Nuri, Preparation of polyurethane wood adhesives by polyols formulated with polyester polyols based on castor oil, Int. J. Adhes. Adhes. 68 (2016) 273–282.
[20] T. Gurunathan, S. Mohanty, S.K. Nayak, Isocyanate terminated castor oil-based polyurethane prepolymer : Synthesis and characterization, Prog. Org. Coat. 80 (2015) 39–48.
[21] N. Bhosale, A. Shaik, S.K. Mandal, Synthesis and characterization of castor oil based hybrid polymers and their polyurethane–urea/silica coatings, RSC Adv. 5 (125) (2015) 103625–103635.
[22] F. Lena do Nascimento Silva, E.M. Schmidt, C.L. Messias, M.N. Eberlin, A.C. Helena Frankland Sawaya, Quantitation of organic acids in wine and grapes by direct infusion electrospray ionization mass spectrometry, Anal. Methods 7 (1) (2015) 53–62.
[23] Y. Soyer, N. Koca, F. Karadeniz, Organic acid profile of Turkish white grapes and grape juices, J. Food Compos. Anal. 16 (5) (2003) 629–636.
[24] G. Rokicki, M. Mazurek, K. Tomczyk, Polyurethane elastomers based on carbonic and tartaric acid derivatives as renewable resources, Polimery 60 (9) (2015) 541–550.
[25] R. Marín, A. Martínez de Ilarduya, S. Muñoz-Guerra, Linear polyurethanes made from naturally occurring tartaric acid, J. Polym. Sci. Part A Polym. Chem. 47 (2009) 2391–2407.
[26] N. Kuramoto, M. Sakamoto, J. Komiyama, T. Iijima, Carboxyl-containing polyesters and polyurethanes from dibenzyl L-tartrate, J. Appl. Polym. Sci. 29 (1984) 977–983.
[27] C.F. Chen, Q. Su, Y.M. Chen, F. Xi, A new optically active polyurethane derived from chiral(2R,3R)(+)-diethyl L-Tartrate and diisocyanate, Chin. J. Polym. Sci. (Engl. Ed.) 17 (4) (1999) 371–373.
[28] J.J.A. Wijs, The Wijs method as the standard for iodine absorption, Analyst 54 (634) (1929) 12.
[29] K.K. Jena, D.K. Chattopadhyay, K.V.S.N. Raju, Synthesis and characterization of hyperbranched polyurethane – urea coatings, Eur. Polym. J. 43 (2007) 1825–1837.
[30] E.E. Gilbert, The unique chemistry of castor oil, J. Chem. Educ. (1941) 338–341.
[31] V.R. Patel, G.G. Dumancas, L.C.K. Viswanath, R. Maples, B.J.J. Subong, Castor oil: properties, uses, and optimization of processing parameters in commercial production, Lipid Insights 9 (1) (2016) 1–12.
[32] A.K. Mishra, D.K. Chattopadhyay, B. Sreedhar, K.V.S.N. Raju, FT-IR and XPS studies of polyurethane-urea-imide coatings, Prog. Org. Coat. 55 (2006) 231–243.
[33] S.S. Panda, B.P. Panda, S. Mohanty, S.K. Nayak, Synthesis and properties of castor oil-based waterborne polyurethane cloisite 30B nanocomposite coatings, J. Coatings Technol. Res. 14 (2) (2017) 377–394.
[34] X. Cao, H. Dong, C.M. Li, New nanocomposite materials reinforced with cellulose nanocrystals in waterborne polyurethane, Biomacromolecules 8 (2007) 899–904.
[35] B. Fernández-D'Arlas,, J.A. Ramos, A. Saralegi, M. Corcuera, I. Mondragon, A. Eceiza, Molecular engineering of elastic and strong supertough polyurethanes, Macromolecules 45 (8) (2012) 3436–3443.
[36] S. Subramani, Y.J. Park, Y.S. Lee, J.H. Kim, New development of polyurethane dispersion derived from blocked aromatic diisocyanate, Prog. Org. Coat. 48 (1) (2003) 71–79.
[37] P. Florian, K.K. Jena, S. Allauddin, R. Narayan, K.V.S.N. Raju, Preparation and characterization of waterborne hyperbranched polyurethane-urea and their hybrid coatings, Ind. Eng. Chem. Res. 4517–4527 (2010).
[38] I.S. Blagbrough, N.E. Mackenzie, A.I. Scott, The condensation reaction between isocyanates and carboxylic acids. A practical synthesis of substituted amides and anilides, Tetrahed. Lett. 27 (11) (1986) 1251–1254.
[39] W.R. Sorenson, Reaction of an isocyanate and a carboxylic acid in dimethyl sulfoxide, J. Org. Chem 24 (2) (1959) 978–980.
[40] G. Socrates, Infrared and Raman Characteristic Group Frequencies, Third, John Wiley & Sons Ltd., Middlesex, 2004.
[41] I. Yilgor, E. Yilgor, I.G. Guler, T.C. Ward, G.L. Wilkes, FTIR investigation of the influence of diisocyanate symmetry on the morphology development in model segmented polyurethanes, Polymer 47 (11) (2006) 4105–4114.
[42] S.S. Panda, B.P. Panda, S. Mohanty, S.K. Nayak, The castor oil based water borne polyurethane dispersion; effect of -NCO/OH content: synthesis, characterization and properties, Green Process Synth. 6 (3) (2016) 341–351.
[43] G. Chen, M. Wei, J. Chen, J. Huang, A. Dufresne, P.R. Chang, Simultaneous reinforcing and toughening: new nanocomposites of waterborne polyurethane filled with low loading level of starch nanocrystals, Polymer 49 (7) (2008) 1860–1870.
[44] H.A. Mohamed, B.M. Badran, A.M. Rabie, S.M.M. Morsi, Synthesis and characterization of aqueous (polyurethane/aromatic polyamide sulfone) copolymer dispersions from castor oil, Prog. Org. Coat. 77 (5) (2014) 965–974.
[45] C. Fu, Z. Zheng, Z. Yang, Y. Chen, L. Shen, A fully bio-based waterborne polyurethane dispersion from vegetable oils: from synthesis of precursors by thiol-ene reaction to study of final material, Prog. Org. Coat. 77 (1) (2014) 53–60.
[46] A. Spyros, D. Anglos, Studies of organic paint binders by NMR spectroscopy, Appl. Phys. A Mater. Sci. Process. 83 (4) (2006) 705–708.
[47] S. Thakur, N. Karak, Castor oil-based hyperbranched polyurethanes as advanced surface coating materials, Prog. Org. Coat. 76 (1) (2013) 157–164.
[48] A.I. Vogel, Vogeĺs Textbook of Practical Organic Chemistry, Fifth, Logman Group, 1989.
[49] V. Garcia-Pacios, V. Costa, M. Colera, J.M. Martin-Martinez, Waterborne polyurethane dispersions obtained with polycarbonate of hexanediol intended for use as coatings, Prog. Org. Coat. 71 (2) (2011) 136–146.
[50] V. García-Pacios, J.A. Jofre-Reche, V. Costa, M. Colera, J.M. Martín-Martínez, Coatings prepared from waterborne polyurethane dispersions obtained with polycarbonates of 1,6-hexanediol of different molecular weights, Prog. Org. Coat. 76 (10) (2013) 1484–1493.
[51] P.A. Steward, J. Hearn, M.C. Wilkinson, Overview of polymer latex film formation and properties, Adv. Colloid Interface Sci. 86 (3) (2000) 195–267.
[52] Kamsons Chemicals PVT. LTD., Water Based Polyurethane Dispersions (PUD's), [Online]. Available: < http://www.kamsons.com/water-based-polyurethane-dispersions.html > (accessed: 01-Mar-2017).
[53] G. Mondragon, A. Santamaria-Echart, M.E.V. Hormaiztegui, A. Arbelaiz, C. Peña-Rodriguez, V. Mucci, M. Corcuera, M.I. Aranguren, A. Eceiza, Nanocomposites of waterborne polyurethane reinforced with cellulose nanocrystals from sisal fibres, J. Polym. Environ. (2017) 1–12.
[54] V. Hormaiztegui, V.L. Mucci, A. Santamaria-Echart, M.A. Corcuera, A. Eceiza, M.I. Aranguren, Waterborne polyurethane nanocomposites based on vegetable oil and microfibrillated cellulose, J. Appl. Polym. Sci. 133 (47) (2016).
[55] V. García-Pacios, M. Colera, Y. Iwata, J.M. Martín-Martínez, Incidence of the polyol nature in waterborne polyurethane dispersions on their performance as coatings on

stainless steel, Prog. Org. Coat. 76 (12) (2013) 1726–1729.
[56] C. Wang, J. Fang, T. Liu, C. Ji, S. Li, Synthesis of waterborne polyurethane dispersions with glycolyzed product from pet waste: effect of hard segment content on its properties, Polym. Sci. Ser. B 57 (5) (2015) 434–443.
[57] L. Lei, Y. Zhang, C. Ou, Z. Xia, L. Zhong, Synthesis and characterization of waterborne polyurethanes with alkoxy silane groups in the side chains for potential application in waterborne ink, Prog. Org. Coat. 92 (2016) 85–94.
[58] H. Fu, Y. Wang, X. Li, W. Chen, Synthesis of vegetable oil-based waterborne polyurethane/silver-halloysite antibacterial nanocomposites, Compos. Sci. Technol. 126 (2016) 86–93.
[59] A. Kaushik, A. Garg, Castor Oil Based polyurethane nanocomposites with cellulose nanocrystallites fillers, Adv. Mater. Res. 856 (2013) 309–313.
[60] S. Lin, J. Huang, P.R. Chang, S. Wei, Y. Xu, Q. Zhang, Structure and mechanical properties of new biomass-based nanocomposite: castor oil-based polyurethane reinforced with acetylated cellulose nanocrystal, Carbohydr. Polym. 95 (1) (2013) 91–99.
[61] Z.S. Petrović, Polymers from biological oils, Contemp. Mater. 1 (1) (2010) 39–50.
[62] V.L. Mucci, A. Ivdre, J.M. Buffa, U. Cabulis, P. Stefani, M.I. Aranguren, Composites made from a soybean oil biopolyurethane and cellulose nanocrystals, Polym. Eng. Sci. (2017).
[63] T. Calvo-Correas, M.A. Mosiewicki, M.A. Corcuera, A. Eceiza, M.I. Aranguren, Linseed oil-based polyurethane rigid foams: synthesis and characterization, J. Renew. Mater. 3 (1) (2015) 3–13.
[64] M.A. Mosiewicki, U. Casado, N.E. Marcovich, M.I. Aranguren, Moisture dependence of the properties of composites made from tung oil based polyurethane and wood flour, J. Polym. Res. 19 (2) (2012).
[65] M.I. Aranguren, I. Rácz, N.E. Marcovich, Microfoams based on castor oil polyurethanes and vegetable fibers, J. Appl. Polym. Sci. 105 (2007) 2791–2800.
[66] K.P. Menard, Dynamic Mechanical Analysis. A Practical Introduction, second ed., CRD Press Taylor & Francis Group, Boca Raton, Florida, USA, 2008.
[67] E. Hablot, D. Zheng, M. Bouquey, L. Avérous, Polyurethanes based on castor oil: kinetics, chemical, mechanical and thermal properties, Macromol. Mater. Eng. 293 (2008) 922–929.
[68] I. Javni, Z.S. Petrovic, A. Guo, R. Fuller, Thermal stability of polyurethanes based on vegetable oils, J. Appl. Polym. Sci. 77 (2000) 1723–1734.
[69] M.N.S. Kumar, Siddaramaiah, Thermogravimetric analysis and morphological behavior of castor oil based polyurethane–polyester nonwoven fabric composites, J. Appl. Polym. Sci. 106 (2007) 3521–3528.
[70] I. Javni, Z.S. Petrović, A. Guo, R. Fuller, Thermal stability of polyurethanes based on vegetable oils, J. Appl. Polym. Sci. 77 (8) (2000) 1723–1734.
[71] M. Lazzari, O. Chiantore, Drying and oxidative degradation of linseed oil, Polym. Degrad. Stab. 65 (2) (1999) 303–313.